



ELSEVIER



# Hydrophobic-core PEGylated graft copolymer-stabilized nanoparticles composed of insoluble non-nucleoside reverse transcriptase inhibitors exhibit strong anti-HIV activity

Anita Leporati<sup>a</sup>, Mikhail S. Novikov<sup>b</sup>, Vladimir T. Valuev-Elliston<sup>c</sup>, Sergey P. Korolev<sup>d</sup>, Anastasia L. Khandazhinskaya<sup>c</sup>, Sergey N. Kochetkov<sup>c</sup>, Suresh Gupta<sup>a</sup>, Julian Goding<sup>a</sup>, Elijah Bolotin<sup>e</sup>, Marina B. Gottikh<sup>d</sup>, Alexei A. Bogdanov Jr.<sup>a,\*</sup>

<sup>a</sup>Laboratory of Molecular Imaging Probes, Department of Radiology, University of Massachusetts Medical School, Worcester, MA

<sup>b</sup>Volgograd State Medical University, Volgograd, Russia

<sup>c</sup>Engelhardt Institute of Molecular Biology, Russian Academy of Sciences, Moscow, Russia

<sup>d</sup>Lomonosov Moscow State University, Belozersky Institute of Physico-Chemical Biology and Chemistry Department, Moscow, Russia

<sup>e</sup>PharmaIN Corp., Bothell, WA

Received 1 April 2016; accepted 11 July 2016

## Abstract

Benzophenone-uracil (BPU) scaffold-derived candidate compounds are efficient non-nucleoside reverse transcriptase inhibitors (NNRTI) with extremely low solubility in water. We proposed to use hydrophobic core (methoxypolyethylene glycol-polylysine) graft copolymer (HC-PGC) technology for stabilizing nanoparticle-based formulations of BPU NNRTI in water. Co-lyophilization of NNRTI/HC-PGC mixtures resulted in dry powders that could be easily reconstituted with the formation of 150–250 nm stable nanoparticles (NP). The NP and HC-PGC were non-toxic in experiments with TZM-bl reporter cells. Nanoparticles containing selected efficient candidate Z107 NNRTI preserved the ability to inhibit HIV-1 reverse transcriptase polymerase activities with no appreciable change of EC50. The formulation with HC-PGC bearing residues of oleic acid resulted in nanoparticles that were nearly identical in anti-HIV-1 potency when compared to Z107 solutions in DMSO (EC50 = 7.5 ± 3.8 vs. 8.2 ± 5.1 nM). Therefore, hydrophobic core macromolecular stabilizers form nanoparticles with insoluble NNRTI while preserving the antiviral activity of the drug cargo.

© 2016 Elsevier Inc. All rights reserved.

**Key words:** Non-nucleoside reverse transcriptase inhibitors; Microbicide; HIV-1; Nanoparticle; Copolymer; Benzophenone-uracil

Increasing the solubility and bioavailability of highly efficient but poorly water-soluble drugs capable of preventing HIV transmission via mucosal barriers presents an important technical challenge. Increasing the water solubility of these drugs through formulation with a carrier provides inroads to the development of

effective anti-HIV preparations capable of penetrating various tissue barriers.<sup>1</sup> Various systems based on nanoparticles (NP) have many desirable properties for mucosal drug delivery, including protection and sustained release of the drug cargo. Moreover, such “nanomedicines” can be biodegradable,

**Abbreviations:** NP, nanoparticle; NNRTI, non-nucleoside reverse transcriptase inhibitor; BPU, benzophenone-uracil; MPEG-gPLL, methoxypoly(ethylene glycol)-graft-N-ε-poly-L-lysine; HC-PGC, hydrophobic core protected graft copolymer; M5P21OL, methoxypoly(ethylene glycol)5000-graft-N-ε-poly-L-lysine (DP 100) acylated with oleic acid; M5P21ST, methoxypoly(ethylene glycol)5000-graft-N-ε-poly-L-lysine (DP100) acylated with stearic acid; M5P21ST, methoxypoly(ethylene glycol)5000-graft-N-ε-poly-L-lysine (DP250) acylated with stearic acid.

Funding has been provided by: 2R01EB000858-10, and the Collaborative Research Partnership grant 1R21 AI108529-01 (to A.B.); Russian Foundation for Basic Research grant 13-04-91440 to M.G.; and Russian Science Foundation grant 14-50-00060 (Chemical synthesis of NNRTI and tests of DNA-dependent RT activity) to S.K. This project was also supported by Awards S10RR027897 and S10RR021043 from the National Center for Research Resources.

\*Corresponding author at: UMMS, Department of Radiology, Worcester, MA.

E-mail address: Alexei.Bogdanov@umassmed.edu (A.A. Bogdanov).

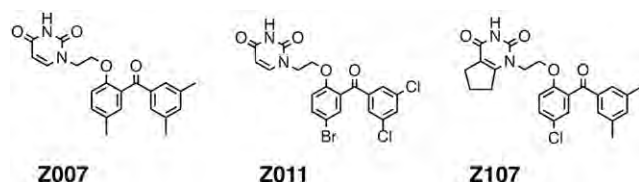


Figure 1. Chemical structures of BPU scaffold-derived NNRTI used in this work. Z007 and Z011 have been previously shown to be efficient NNRTI,<sup>18</sup> while Z107 is new to this study.

biocompatible and functionalized depending on proper material selection and manufacturing.<sup>2</sup> A variety of nano-architectures (i.e. liposomes, dendrimers, polymeric NP, nanocrystals, nanofibers and inorganic NP) are being explored as formulations for novel microbicide candidates.<sup>3–5</sup> Taking into account the NP composition, all NP-based systems designed so far for anti-HIV microbicidal applications can be divided into two major groups: 1) NP formed by components that have intrinsic antiretroviral activity<sup>6,7</sup>; 2) NP containing a cargo with antiretroviral activity, which is combined and stabilized with certain carrier molecules such as poly(lactic-co-glycolic acid) (PLGA) and PLGA blends,<sup>8–11</sup> as well as other polymeric carriers.<sup>12–14</sup> Despite promise in pre-clinical studies, the majority of nano-formulated microbicides so far have not succeeded in clinical trials, thus it is imperative to continue investigations of new formulations by using improved in vitro testing algorithms<sup>15</sup> as well as human and animal mucosal models.<sup>16,17</sup>

In this vein the goal of our work was to obtain and test stabilized water-soluble nano-formulations of a novel family of highly efficient but insoluble non-nucleoside reverse transcriptase inhibitors (NNRTI)<sup>18,19</sup> (Figure 1) for their application as potential microbicides.

## Methods

Syntheses of NNRTI and hydrophobic-core MPEG-gPLL are described in the Supplementary Materials.

### Formulation of NNRTI with HC-PGC

Three NNRTI (Figure 1) were tested in our work: two N1-alkylated uracil derivatives bearing  $\omega$ -(2-benzyl- and 2-benzoylphenoxy)alkyl substituents, i.e. Z007 1-(2-(2-(3,5-dimethylbenzoyl)-4-methylphenoxy)ethyl)pyrimidine-2,4(1H,3H)-dione; and Z011 1-(2-(4-bromo-2-(3,5-dichlorobenzoyl)phenoxy)ethyl)pyrimidine-2,4(1H,3H)-dione, were described before<sup>18</sup> and one, i.e. Z107 1-(2-(4-chloro-2-(3,5-dimethylbenzoyl)phenoxy)ethyl)-1,5,6,7-tetrahydro-2H-cyclopenta[d]pyrimidine-2,4(3H)-dione has not yet been tested extensively. The NNRTI were used as HPLC-purified dry powders which were dissolved at 65 °C in dry tert-butyl alcohol at a concentration of 1 mM. Solutions of HC-PGC (10 mg/ml) in tert-butyl alcohol were mixed with various volumes of NNRTI to achieve ratios from 1:40 to 3:20 (NNRTI/HC-PGC, by weight) and kept at 65 °C with periodic mixing for 30 min. The solutions were then rapidly frozen and lyophilized. The obtained powder was stored under argon. To reconstitute the formulations in water, the powder was rapidly

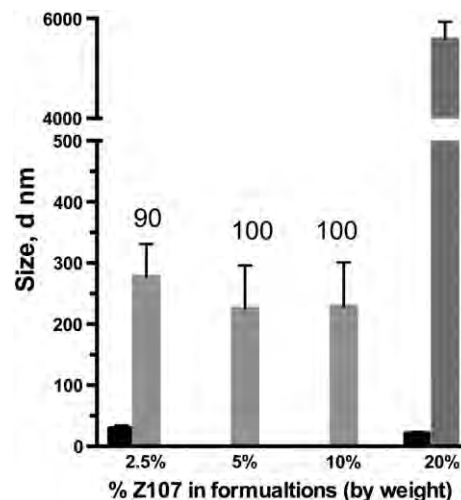


Figure 2. The dependence of NP sizes (shown as number average diameters, mean  $\pm$  SD) on the content of Z107 NNRTI in the formulation with HC-PGC (M5P21OL, 10 mg/ml) as determined by dynamic light scattering (Zetasizer Nano ZS, Malvern Inst). The content of the main fraction in formulations is shown above the bars in gray. The remaining fraction of free (non-incorporated) MPEG-gPLL NP is shown as black bars.

vortexed after adding hot (75 °C) 10 mM Hepes, 0.15 M NaCl, pH 7.2 to obtain a colloidal solution containing 10 mg/ml HC-PGC that stabilized various amounts of NNRTI. After equilibrating at 65 °C for 1 h the solutions were cooled at room temperature and analyzed using dynamic light scattering (Zetasizer Nano ZS, Malvern Instruments, Westborough, MA).

### Testing in recombinant HIV-1 RT enzyme system

DNA-dependent DNA polymerase activity of HIV RTs was tested by using 0.75  $\mu$ g of activated calf thymus DNA, 0.05  $\mu$ g p66/p66 RT, 3 IM dATP, 30  $\mu$ M of dCTP, dGTP and dTTP, 1  $\mu$ Ci [ $\alpha$ -<sup>32</sup>P]dATP in a Tris–HCl buffer (50 mM, pH 8.1) containing also 10 mM MgCl<sub>2</sub>, and 0.2 M KCl. RNA-dependent DNA polymerase and RNase H activity assay of HIV-1 RT were tested by using 100 nM duplex composed of an 18-mer oligoribonucleotide (18-Ribo-FI: 5'-rGA UCUGAGCCUGGGAGCU-fluorescein-3') and a 15-mer oligodeoxyribonucleotide (15-[<sup>32</sup>P]-deoxy: 5'-[<sup>32</sup>P]AGC TCCCAGGCTCAG-3'). Reaction mixtures consisted of 15  $\mu$ L of 50 mM Tris/HCl pH 8.0, containing 200 mM KCl, 100 mM MgCl<sub>2</sub>, 100 nM p66/p51 RT to which various concentrations of inhibitors were added followed by a 15 min incubation at 37 °C. The reaction was stopped by adding 80  $\mu$ L of 7 mM EDTA, 0.375 M sodium acetate, 10 mM Tris–HCl, pH 8, 0.125 mg/ml glycogen. The mixture was extracted by phenol/chloroform, and DNA fragments were precipitated with ethanol. The reaction products were separated by electrophoresis in a 20% polyacrylamide/7 M urea gel. Gel images were recorded using a phosphorimager in fluorescence mode to determine the presence of RNase H activity and radioactivity mode for RNA-dependent DNA-polymerase activity. Images were then quantified using Quantity One 4.6.6. (Bio-Rad, USA).

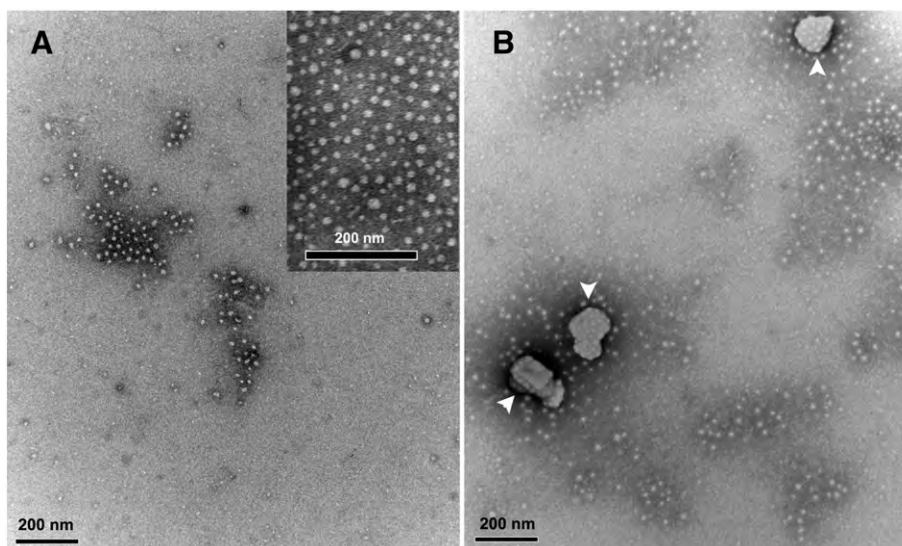


Figure 3. Transmission electron microscopy of M5P21OL (1 mg/ml, **A**) and Z107-M5P21OL (2.5% NNRTI by weight, **B**), at 1 mg/ml M5P21OL after staining/fixation with uranyl acetate. Arrowheads point to stabilized crystalline NP of Z107. The inset in A shows M5P21OL NP at 128,000 $\times$ . The bar = 200 nm.

#### HIV-1 inhibition assays

The HIV-1 CCR5-tropic antiviral assay in MAGI-CCR5 cells was performed after the co-addition of test compounds and HIV-1 to the target cells; CD4-dependent CCR5-tropic HIV-1 cell-to-cell transmission assay was performed by using MOLT4/R5 effector cells and GHOST<sup>3</sup> R5 CD4-positive target cells as described in<sup>15</sup> (Infectious Disease Research Department, Southern Research Contractor, Frederick, MD). All other assays were performed by using TZM-bl cells stably expressing CD4/CCR5 and bearing integrated copies of the luciferase cDNA under control of the HIV-1 LTRs (NIH AIDS Research and Reference Reagent Program). Cells were maintained in 10% fetal bovine serum/DMEM (Thermo Fisher Scientific); HIV-1IIIIB virus (NIH AIDS Research and Reference Reagent Program) was propagated in H9-HTLV-III CC 1983 cells cultured in 10% fetal bovine serum, RPMI1640 with l-glutamine (Gibco, ThermoFisher Scientific) until the concentration of p24 corresponding to the virion content of  $3 \cdot 10^6$ – $3 \cdot 10^7$  infectious units or 24–34 ng p24/ml was achieved as determined by a p24 ELISA assay (QuickTiter Lentivirus Titer Kit, Clontech). Virus stocks were obtained after removing cell debris by centrifugation and stored frozen at  $-80^\circ\text{C}$ . Adherent TMZ-bl cells ( $10^5$ /well 96-well plates) were washed with fresh medium and infected by using 3.65 ng HIV-1 p24/well for 2 h. The supernatant was then removed and adherent cells were treated for 24 h with serially diluted BPU test compounds (Z007, Z011 and Z107, from 2 mM solutions in DMSO) or their complexes with HC-PGC carriers in complete cell culture medium. In some experiments, Nevirapine and Efavirenz (provided by NIH AIDS Research and Reference Reagent Program) were used for comparison. Three days post infection, cells were lysed and were tested for luciferase activity using luciferin/ATP reagent (Promega) using SpectraMAX M5 plate reader (Molecular Devices). The obtained results were analyzed and fitted using log(inhibitor)vs. response routine (equation  $Y = \text{Bottom} + (\text{Top}-\text{Bottom})/(1 + 10^{-(X-\text{LogEC50})})$ )

using Prism 6.0 software (Graph Pad Software Inc.). Toxicity to cells was determined by using WST-1 (Roche) after treating cells with NNRTI and their formulations with HC-PGC for 4 h.

#### Microscopy

High-resolution transmission electron microscopy (TEM) characterization of NP was performed by incubating NP at a dilution with 1:10 phosphate-buffered saline(Ambion) on formvar-coated grids stabilized with evaporated carbon film with negative staining with 1% uranyl acetate and further examining the grids under EM (FEI Tecnai 12 Spirit, at 5–128,000 $\times$  magnification). Fluorescence microscopy was performed using Leica TCS SP5 II laser scanning confocal microscope using laser lines at 405 (DAPI) and 488 (AlexaFluor 488) nm.

## Results

#### Copolymers with hydrophobic core

We synthesized and used as NP stabilizers various hydrophobic core MPEG-gPLL (MPEGylated-graft-poly-l-lysine)copolymers by using a scheme that does not require purification of the intermediates (improved synthesis and purification of MPEG-gPLL intermediate graft copolymer have been reported previously<sup>20</sup>). The synthesis included two consecutive covalent modifications of PLL backbone N- $\epsilon$ -amino groups with activated esters of MPEG-carboxylic acid and fatty acid residues (C18:0 stearic acid and C18:1 cis-9 oleic acids were used in this work).<sup>21</sup> Initially we tested two PLL with different chain lengths for covalent modification, i.e. we used 50% MPEGylation of a shorter PLL with degree of polymerization DP = 100 and 25% MPEGylation for PLL with DP = 250. Both fatty-acid acylated products had excellent solubility in water, chloroform and tert-butanol. We determined that 25% covalent modification of amino groups with MPEG5000 (as determined by TNBS assay) was sufficient for

Table 1  
Properties of fatty acid-acylated MPEG-gPLL (HC-PGC) and NNRTI/HC-PGC NP solutions obtained by using various NNRTIs and HC-PGC stabilizers.

Sample	Z-average (nm), and number-corrected hydrodynamic diameter $\pm$ SD, nm	PDI	Zeta-potential (mV)
M5P21OL*	30.5; 15.6 $\pm$ 4.2	0.3	-5.4
M5P21ST (modification - 50% MPEG)	36.2; 23.4 $\pm$ 6.3	0.1	-7.7
M5P52ST (modification - 25% MPEG)	35.7; 19.5 $\pm$ 5.9	0.1	-3.7
Z007-M5P21ST (5% NNRTI by weight)	151.6; 105 $\pm$ 24	0.3	-1.0
Z007-M5P52ST (5% NNRTI by weight)	129.0; 225 $\pm$ 97	0.5	-1.5
Z011-M5P21OL (5% NNRTI by weight)	206.0; 246 $\pm$ 79	0.3	-2
Z107-M5P21OL (5% NNRTI by weight)	272.0; 226 $\pm$ 72	0.4	-1.0
Z107-M5P21ST (5% NNRTI by weight)	370.0; 155 $\pm$ 62	0.5	-1.2
Z107-M5P52ST (5% NNRTI by weight)	310.0; 353 $\pm$ 97	0.5	-1.0

\* M5, methoxy poly(ethylene glycol)5000 carboxylate; PL, poly-L-lysine; OL, oleoyl; ST, stearoyl.

water solubility of the resultant hydrophobic core copolymers regardless of their PLL backbone chain length. As determined by  $^1\text{H}$  NMR spectroscopy, the average content of MPEG chains and fatty acid chains in the obtained HC-PGC after the purification using ultrafiltration was as follows: MPEG5-PLL21-stearoyl (M5P21ST) – per one backbone PLL ( $n = 100$ ): 30 residues of MPEG5000, 50 stearic acid residues; MPEG5-PLL21-oleoyl (M5P21OL) – per one PLL ( $n = 100$ ): 38 residues of MPEG5000, 70 oleic acid residues; MPEG5-PLL52-stearoyl (M5P52ST) – per one PLL ( $n = 240$ ): 56 residues of MPEG5000, 65 stearic acid residues. The results of  $^1\text{H}$  NMR spectroscopy indicate that the final composition of HC-PGC has been affected by removal of a smaller (and less PEGylated) fraction of HC-PGC, which was eliminated during the ultrafiltration.

#### NNRTI formulation with HC-PGC

Excellent solubility of both NNRTI and HC-PGC in tert-butanol allowed complete co-solubilization of HC-PGC and NNRTI that was followed by snap-freezing and lyophilization. After the solubilization of lyophilized solids in HBS (25 mM HEPES, 0.125 M NaCl, pH 7.5) the compositions were subjected to size measurements by using laser light scattering (photon correlation spectroscopy, LALLS) and electron microscopy (Figures 2 and 3). HC-PGC molecules had average diameters of 10–30 nm depending on the length of the PLL backbone and MPEGylation degree (Table 1). While NNRTI lyophilized from tert-butanol alone did not form any stable water dispersions in the absence of HC-PGC copolymer, the mixed compositions consisting of approximately 5–10% NNRTI of the total weight of the formulation (0.5–1 mg/ml NNRTI) formed NP in water or buffer solution after reconstitution at 65 °C. The range of appropriate NNRTI content in the NP was determined by using Z107 candidate drug. We observed facile formation of stable NP that was feasible at the ratios of NNRTI that did not exceed 30:1 (NNRTI/HC-PGC, mol/mol, Figure 2). Measurements of average diameter changes of the stabilized NP solutions over time showed that at 5% of NNRTI by weight (i.e. at the concentration of 1–1.5 mM NNRTI in nano-formulations) the obtained colloidal solutions were stable at room temperature for at least 2 months with no changes in average diameters (Zav). The results of LALLS and particle charge measurements are shown in Table 1 using all three NNRTI. Overall, in NP solutions that contained between 5 and 10% of NNRTI by weight we

observed unimodal submicron particle size distributions that were dependent on individual NNRTI and the type of stabilizer. Depending on HC-PGC, we obtained NP in the range of 150–370 nm and relatively high polydispersity indices (PDI = 0.3–0.5). Electron microscopy of uranyl acetate-stained HC-PGC revealed 15–25 nm spherical particles (Figure 3, A) confirming the results of dynamic light scattering (Table 1). The NNRTI-containing NP formed in the presence of HC-PGC appeared irregularly shaped and crystalline with maximum dimensions in the range of 200–300 nm and with most of NNRTI NP carrying multiple smaller adsorbed HC-PGC nanoparticles (Figure 3, B). All HC-PGC stabilized NNRTI NP showed a wide distribution of zeta potentials, and displayed an overall weak negative charge of the particles (Table 1). However, multiple MPEG chains were present on the surface of NP creating a steric barrier. As a result, the stability of HC-PGC-stabilized NNRTI NP (i.e. the observed lack of aggregation) did not correlate with their low zeta potential, which would usually suggest low stability. Since formulating NNRTI with M5P21OL resulted in lower polydispersity than other tested HC-PGC, we chose this NP stabilizer for our further in vitro experiments.

#### Testing in recombinant HIV-1 RT system

The second phase of BPU/HC-PGC testing included determining whether BPU still inhibit reverse transcriptase activity after formulating into stabilized NP. Two NNRTI (BPU Z007 and Z011) have already been tested as inhibitors of RNA-dependent DNA polymerase as well as DNA-dependent DNA polymerase activities of HIV-1 RT,<sup>18</sup> both of which are essential for retroviral replicative cycle. To perform EC50 measurements in solutions containing purified enzyme subunits, NNRTI had to be dissolved in DMSO while NNRTI/HC-PGC did not contain any organic solvents. We used recombinant heterodimeric (p66/p51) wild type RT as well as homodimeric (p66/p66) mutant RT enzymes to determine 1) whether NNRTI activity had been preserved after formulating into the stabilized NP and 2) whether any of the tested NNRTI still retained wide spectrum activity against the drug-resistant variants of the enzyme. First, the carrier/stabilizer molecule itself, i.e. various HC-PGC showed no effect on RT activities at concentrations that were more than 10-fold higher than those used for testing NNRTI/HC-PGC formulations. Second, we have elucidated that

Table 2  
RT Inhibition with NNRTI and NNRTI/HC-PGC nanoparticles.

Test compound	HIV-1 reverse transcriptase	RNA-dependent DNA polymerization, IC <sub>50</sub> (μM)		DNA-dependent DNA polymerization, IC <sub>50</sub> (μM)	
		From DMSO stock solution	Complex with HC-PGC	From DMSO stock solution	Complex with HC-PGC
Z107	Wild type	3 ± 1	5 ± 1	0.7 ± 0.2	0.5 ± 0.1
	L100I	10 ± 3	15 ± 4	3 ± 1	1.5 ± 0.2
	K103N	40 ± 10	100 ± 30	70 ± 2	95 ± 15
	V106A	>100	>100	>100	>100
	Y181C	5 ± 2	40 ± 10	6 ± 2	1.9 ± 0.5
	G190A	35 ± 10	70 ± 20	45 ± 15	0.9 ± 0.3
	K103N + Y181C	80 ± 30	100 ± 20	50 ± 20	9 ± 2
Z011	Wild type	–	–	0.7 ± 0.1	1.2 ± 0.4
	L100I	–	–	1.8 ± 0.6	>100
	K103N	–	–	6 ± 1	>100
	V106A	–	–	>100	>100
	Y181C	–	–	1.4 ± 0.5	22 ± 5
	G190A	–	–	1.6 ± 0.3	2.6 ± 0.7
	K103N + Y181C	–	–	10 ± 3	>100
Z007	Wild type	50 ± 20	100 ± 20	40 ± 10	8 ± 2
	L100I	100 ± 30	>100	>100	>100
	K103N	>100	>100	>100	>100
	V106A	>100	>100	>100	>100
	Y181C	>100	>100	>100	>100
	G190A	>100	>100	>100	>100
	K103N + Y181C	>100	>100	>100	>100

none of the NNRTI/HC-PGC complexes inhibited the RNase H activity of RT at concentrations up to 300 μM. The results of the inhibition of RT polymerase activities are shown in Table 2. The data demonstrated that overall, there was a preservation of activity against the wild type of RT for all NNRTI tested after their formulation with M5P21OL. Moreover, NNRTI complexes mostly remained active against drug-resistant variants of RT with the exception of Z007, which also showed low activity in DMSO solutions. The two most remarkable findings were that: 1) NNRTI Z107 showed a very good profile of inhibitory activity in the case of a double mutant (K103N+Y181C) enzyme (EC<sub>50</sub> value for double mutation observed for Z107 complex are 9 ± 2 μM for DNA-dependent DNA polymerization assay); and 2) the G190A mutation, the main reason for nevirapine resistance, did not result in resistance to Z107 (IC<sub>50</sub> < 1 μM) and Z011 (IC<sub>50</sub> = 2.6 ± 0.7 μM). G190A mutation in HIV-1 RT apparently requires a “horseshoe” mode of binding of the inhibitor into the mutant binding pocket of the enzyme.<sup>22</sup>

#### Antiviral activity

To test whether HC-PGC stabilized NP formulations of NNRTI preserved their ability to inhibit HIV-1 infection, we compared the antiviral properties of all three insoluble NNRTI (Z007, Z011 and Z107) as solutions in DMSO or after formulating these NNRTI into NP by using HC-PGC. We initially performed a 2 h infection of TZM-bl reporter cells with HIV-1 and then treated the already infected cells with the inhibitor. To decrease the potential non-specific effects on cells, we limited the exposure to NNRTI formulations to 24 h. The results demonstrating the effect of HC-PGC carriers alone on HIV-1IIIIB infection and the inhibition of infection by NNRTI (either free or HC-PGC-formulated) using reporter TZM-bl cells are shown in Figure 4, and the obtained EC<sub>50</sub> and toxicity results

are summarized in Table 3. There were no toxic effects on TZM-bl cells detectable at the concentrations of NNRTI exceeding EC<sub>50</sub> over 500 times. The only toxic effect attributable to DMSO solvent was observed in the case of free NNRTI at the concentration of 100 μM. While NP-stabilizing HC-PGC molecules did not show any concentration-dependent inhibition of HIV-1 infection within a wide range of concentrations (including the concentration of HC-PGC corresponding to that of the formulated NNRTI NP, Figure 4, A), the NP of all three experimental drugs showed concentration-dependent inhibition of HIV-1 infection of TZM-bl cells (Figure 4, B). Overall, as determined by calculating EC<sub>50</sub> values, the stabilization of NNRTI in water solutions with oleic acid-modified HC-PGC resulted in a 2–3 fold increase of EC<sub>50</sub> in the case of Z011 and Z007 and had no effect on anti-HV-1 activity of the most efficient Z107 inhibitor. The EC<sub>50</sub> of Z107 NP formulation with M5P21OL was similar to the drug alone (8.2 ± 5.1 vs. 7.5 ± 3.8 nM). The stabilization of NP with HC-PGC bearing stearic acid residues (M5P21ST) in its core instead of oleic acid (M5P21OL) showed a more pronounced increase of EC<sub>50</sub> (up to 10 times) in the case of Z107 and Z011. Since Z107 and its formulation with HC-PGC carriers showed high specificity indices (i.e. low toxicity to cells in addition to high anti-HIV-1 efficacy), a standard co-addition experiment was performed by using either Z107 or Z107 NP in a CCR5-tropic HIV-1 Ba-L antiviral assay in MAGI-CCR5 cells (Table 3). The co-addition of HIV-1 and the NNRTI revealed that Z107-M5P21OL NP and Z107 have similar anti-HIV-1 activities with EC<sub>50</sub> of 3 nM. Consistent with this finding were the observed similar efficacies of both free Z107 and Z107-M5P21OL NP in preventing CCR5-tropic HIV-1 transmission from infected MOLT4/R5 cells to GHOST<sup>3</sup> R5 target cells (Table 3).

Confocal fluorescence microscopy of TZM-bl cells incubated either with AF488-labeled HC-PGC, or fluorescent NNRTI NP

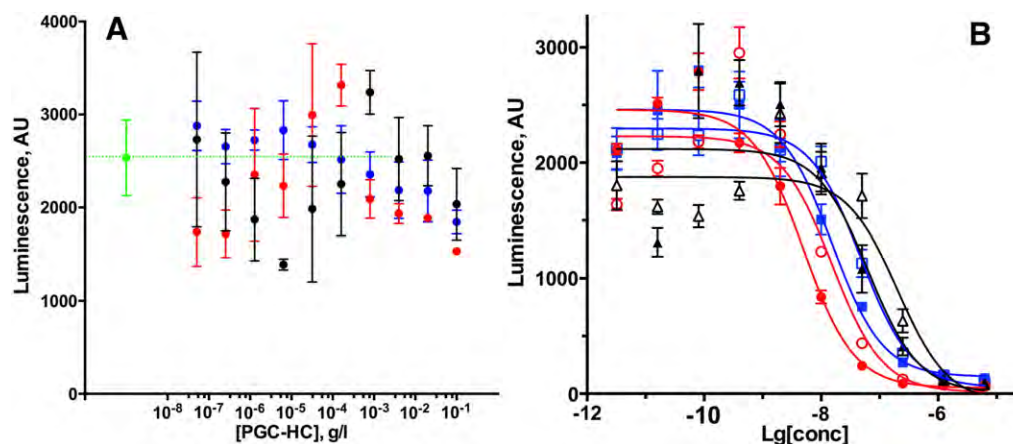


Figure 4. Dependence of TzM-bl HIV-1 infection on the concentration of HC-PGC carriers alone (A) or NNRTI and NNRTI/HC-PGC (B). A- M5P21OL (black circles), M5P21S (red circles), M5P252S (blue circles). B- Titration of NNRTI was performed either from a stock solution of NNRTI in DMSO - solid symbols, or after formulating NNRTI using HC-PGC (M5P21OL) - open symbols. Z107 - red; Z011 - blue; Z007 - black. Inhibition of HIV-1 infection of TzM-bl cells determined by using fLuc expression luminescence assay. Data is shown as mean  $\pm$  SD. The obtained EC<sub>50</sub> values are summarized in Table 3.

(Figure 5) demonstrated evidence of water-phase uptake of the HC-PGC carrier molecules (pinocytosis, Figure 5, A). NNRTINP stabilized with AF488-labeled HC-PGC showed uptake via endocytosis after the adsorption of NP on the plasma membrane surface (Figure 5, D), which was clearly visible alongside with cytoplasmic fluorescence in the case of HIV-infected cells. Non-infected cells demonstrated less active binding and internalization of NP (Figure 5, C).

## Discussion

We studied NP-based formulation and properties of NNRTI inhibitors that belong to the benzophenone-uracyl (BPU) scaffold-derived NNRTI (Figure 1) family. These NNRTI are attractive active microbicide candidates since they have been previously proven efficient in tests involving both HIV-1 RT as well as its mutant forms, including a double mutant (K103N + Y181C).<sup>18</sup> However, similar to many other first- and second- generation NNRTI (reviewed in<sup>23</sup>), BPU are poorly soluble in water essentially limiting their efficacy in applications involving HIV-infected cells. We hypothesized that their solubility could be increased after their complex formation with carriers formulated using hydrophobic core protected graft copolymer (HC-PGC) technology. This graft copolymer has MPEG chains covalently linked to a polyamino acid (such as poly-L-lysine) backbone, which is then acylated with long-chain fatty acids at side chain amino groups. HC-PGC has been initially developed for transient binding of bio-active peptides for improving their PK, e.g. for designing a long-acting native GLP-1 formulation for type 2 diabetes therapy.<sup>24,25</sup> We decided to expand the potential applications of this technology to provide a component that affords stabilization of poorly water-soluble low molecular weight drugs instead of peptides. For penetrating mucosal barriers, microbicide formulations must be small enough to avoid steric obstruction and have a hydrophilic, neutral surface to avoid adhesion. Amphiphilic

HC-PGC molecules are potentially capable of providing PEG surface coating, which has been shown to be important for efficient mucus penetration. It has been demonstrated that 100 nm-1  $\mu$ m polystyrene particles were escaping adhesive entrapment in fresh undiluted human cervicovaginal mucus (CVM) if they were densely PEGylated.<sup>26</sup> Furthermore, PLGA particles as large as 500 nm were shown to diffuse rapidly through undiluted CVM if densely coated with low molecular weight PEG.<sup>27</sup> We assumed that HC-PGC is capable of providing such dense coating. Therefore, we studied the initial optimization and testing of the BPU/HC-PGC formulations in experiments performed with a panel of recombinant RT enzymes as well as a comparative testing of anti-HIV-1 activity of water-soluble formulations in TzM-bl cells.<sup>28,29</sup> As we initially anticipated the stabilized nanoparticles formulated by using one of the most active experimental NNRTI (Z107) preserved an ability to inhibit polymerase activity of wild-type and mutant HIV-1 RT and in some cases, based on EC<sub>50</sub> measurements NP exceed the inhibitory activity of DMSO-solubilized drug (Table 2). The experiments in TzM-bl cell culture confirmed that NP containing Z107 were efficient in preventing the infection of effector cells in medium-to-low nanomolar range. The low toxicity of NP (CC<sub>50</sub> above 100  $\mu$ M, Table 3) and very low nM range of Z107 NP EC<sub>50</sub> indicate very high selectivity of this nano-formulation (TI > 12,000) in the case of infected TzM-bl assay and in the case of HIV-1 Ba-L replication inhibition after the drug co-addition together with the virus (TI > 166).

However, it should be noted that the EC<sub>50</sub> values clearly depended on HC-PGC stabilizer composition suggesting critical importance of the stabilizer design. The modification of MPEG-gPLL with saturated stearic acid (e.g. M5P21ST-stabilized NP) resulted in less strong inhibitory activity of Z107 NP than the modification with unsaturated oleic acid. This result suggests either a stronger interaction of NNRTI with stabilizing molecules in the case of unsaturated fatty acid (which results in lower effective concentration of the free drug

Table 3  
Anti-HIV1 activity of free NNRTI and HC-PGC stabilized nanoparticles containing NNRTI.

NNRTI	HC-PGC	HIV-1IIIIB Inhibition, EC50 nM <sup>b</sup>	HIV-1 Ba-L inhibition, EC50 (EC90), nM <sup>c</sup>	CD4-dependent CCR5-tropic HIV-1 cell-to-cell transmission inhibition assay, EC50 (EC90),nM <sup>d</sup>	Toxicity CC50, μM <sup>e</sup>	Therapeutic index, TI <sup>e</sup>
Z107	- <sup>a</sup>	7.5 ± 3.8	3.0 (30)	40.0 (150)	>50	>6000
	M5P21OL	8.2 ± 5.1	3.0 (20)	<32.0 (150)	>100	>12,000
	M5P21ST	110 ± 10	-	-	>100	>900
Z011	- <sup>a</sup>	25.5 ± 7.6	-	-	>50	>1900
	M5P21OL	55.6 ± 16.4	-	-	>100	>1800
	M5P21ST	210 ± 13	-	-	>100	>470
Z007	- <sup>a</sup>	54.4 ± 7.5	-	-	>50	>920
	M5P21OL	140.6 ± 82.6	-	-	>100	>700
	M5P21ST	150 ± 10	-	-	>50	>300

<sup>a</sup> The dose–response semi-logarithmic plots were used for calculating half-maximal and 90% effective concentrations (EC50 and EC90). Dilutions of Z107 in the absence of HC-PGC were made from DMSO stock solutions;

<sup>b</sup> Mean ± SD, n = 3 independent titrations;

<sup>c</sup> The assay performed using MAGI CCR5-tropic HIV-1 infection assay after the co-addition of test compounds and HIV-1 to the cells;

<sup>d</sup> CD4-dependent CCR5-tropic HIV-1 cell-to-cell transmission assay was performed by using MOLT4/R5 effector cells and GHOST<sup>(3)</sup>R5 CD4-positive target cells;

<sup>e</sup> 50% cytotoxic concentrations (CC50) were determined by using WST-1 test. No toxicity was recorded below indicated concentrations. Therapeutic indices were determined as TI = CC50/EC50.

in water), or a creation of more efficient steric barrier preventing cellular uptake of stabilized NP. Since the use of unsaturated longer chain fatty acid has a potential disadvantage of auto- and photo-oxidation, further optimization of fatty acid chain length such as the use of shorter saturated fatty acids (e.g. myristic acid) may potentially result in NP with properties similar to unsaturated oleic acid. Furthermore, by using confocal microscopy we observed the plasma membrane binding and uptake of fluorescent labeled Z107 NP along the surface of HIV-1 infected TZM-bl cells while no such binding was present in the case of HC-PGC alone, which apparently was taken up by the cells only from water phase. The detailed pathways of stabilized NNRTI NP uptake by cells are currently under investigation. A recent report suggests the involvement of lipid rafts in this process,<sup>30</sup> which may potentially indicate the observed preference in fatty acid composition of the cellular uptake pathways. One of the potential limitations of our study is that HeLa-derived cells (i.e. epithelioid carcinoma-derived MAGI and TZM-bl) are model cell lines and thus are different from the natural human cell targets of HIV-1 infection. However, HeLa-derived cell lines are currently adopted for use in a standard microbicide-testing algorithm.<sup>15</sup> Since these model cell lines are expressing high numbers of CD4 and CCR5 they are maximally sensitive to HIV-1 infection. It also should be noted that Z107 nano-formulations already showed promise in non-HeLa based tests since they were efficient in HIV-1 transmission inhibition assay that involved HIV-1-producing effector cells and GHOST<sup>3</sup> R5 CD4-positive target cells (Table 3). It is highly likely that differences in drug-cell interactions and tissue barriers will affect the outcomes in real viral targets. Further testing in human mucosal tissue explants<sup>31</sup> or in rodents with partially reconstituted elements of human immune system<sup>16,32</sup> should provide more realistic estimates of anti-HIV-1 efficacy. The use of more realistic testing systems and algorithms will also provide an opportunity to explore novel modifications of stabilizer HC-PGC molecules that could carry various

additional drug payloads including antibodies for specific targeting to human cells.<sup>33</sup>

In conclusion, our results indicate that the formulations obtained after the reconstitution of water-insoluble NNRTI in the presence of HC-PGC retain their inhibitory activity against wild-type RT and key mutant RTs. One promising candidate NNRTI (Z107) has been identified in these RT activity inhibition tests. By formulating Z107 together with M5PL21OL we obtained stable NP with average diameters of 100–250 nm that allow NNRTI to reach high concentrations in a water-miscible form. Anti HIV-1 infection tests in reporter cells demonstrated that this formulation preserves RT and anti-HIV-1 activity of the parent NNRTI drug. The developed NP formulation strategy may be considered as a promising route for developing potent candidates for use as effective topical microbicides that prevent the spread of HIV infection due to the high selectivity of their anti-retroviral effect.

### Acknowledgment

Funding has been provided by:2R01EB000858-10, and the Collaborative Research Partnership grant 1R21 AI108529-01 (to A.B.); Russian Foundation for Basic Research grant 13-04-91440 to M.G.; and Russian Science Foundation grant 14-50-00060 (Chemical synthesis of NNRTI and tests of DNA-dependent RT activity) to S.K. This project was also supported by Awards S10RR027897 and S10RR021043 from the National Center for Research Resources.

### Appendix A. Supplementary data

Supplementary data to this article can be found online at <http://dx.doi.org/10.1016/j.nano.2016.07.004>.

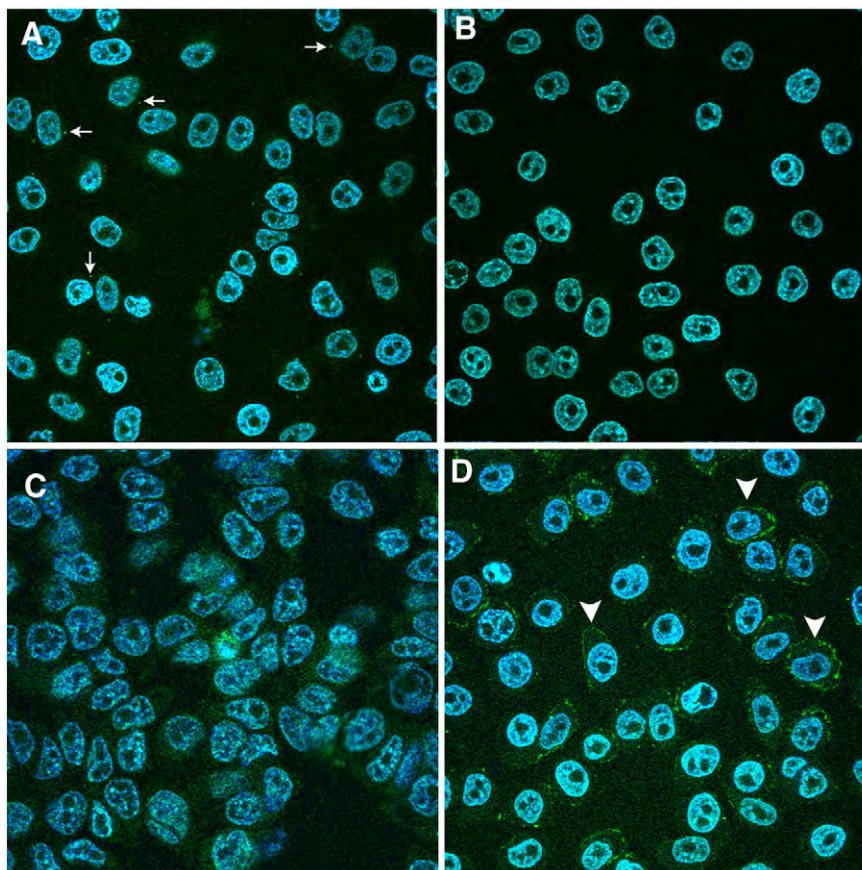


Figure 5. Confocal microscopy of control (A,C) or HIV-1 infected (B,D) TZM-bl cells. Cells were incubated for 24 h with AF488-labeled HC-PGC carrier only (1 mg/ml M5P21OL) (A,B) or with Z107 NNRTI/M5P21OL NP (0.1 mg/ml Z107, 1 mg/ml M5P21OL) (C,D). Blue - DAPI, green - AF488. Large pinosomes are marked with arrows, NP within the peri-membrane compartment and NP adsorbed on plasma membrane are shown with arrowheads.

## References

- Kanmogne GD, Singh S, Roy U, Liu X, McMillan J, Gorantla S, et al. Mononuclear phagocyte intercellular crosstalk facilitates transmission of cell-targeted nanoformulated antiretroviral drugs to human brain endothelial cells. *Nanomedicine* 2012;**7**:2373-88.
- Edagwa BJ, Zhou T, McMillan JM, Liu XM, Gendelman HE. Development of HIV reservoir targeted long acting nanoformulated antiretroviral therapies. *Curr Med Chem* 2014;**21**:4186-98.
- Ensign LM, Cone R, Hanes J. Nanoparticle-based drug delivery to the vagina: a review. *J Control Release* 2014;**190**:500-14.
- du Toit LC, Pillay V, Choonara YE. Nano-microbicides: challenges in drug delivery, patient ethics and intellectual property in the war against HIV/AIDS. *Adv Drug Deliv Rev* 2010;**62**:532-46.
- Sanchez-Rodriguez J, Vacas-Cordoba E, Gomez R, De La Mata FJ, Munoz-Fernandez MA. Nanotech-derived topical microbicides for HIV prevention: the road to clinical development. *Antivir Res* 2015;**113**:33-48.
- Price CF, Tyssen D, Sonza S, Davie A, Evans S, Lewis GR, et al. Spl7013 gel (Vivagel®) retains potent HIV-1 and HSV-2 inhibitory activity following vaginal administration in humans. *PLoS One* 2011;**6**:e24095.
- McGowan I, Gomez K, Bruder K, Febo I, Chen BA, Richardson BA, et al. Phase I randomized trial of the vaginal safety and acceptability of Spl7013 gel (Vivagel) in sexually active young women (mtn-004). *AIDS* 2011;**25**:1057-64.
- Destache CJ, Belgum T, Christensen K, Shibata A, Sharma A, Dash A. Combination antiretroviral drugs in p1ga nanoparticle for HIV-1. *BMC Infect Dis* 2009;**9**:198.
- Steinbach JM, Weller CE, Booth CJ, Saltzman WM. Polymer nanoparticles encapsulating sima for treatment of HSV-2 genital infection. *J Control Release* 2012;**162**:102-10.
- Belletti D, Tosi G, Forni F, Gamberini MC, Baraldi C, Vandelli MA, et al. Chemico-physical investigation of tenofovir loaded polymeric nanoparticles. *Pharm* 2012;**436**:753-63.
- Ham AS, Cost MR, Sassi AB, Dezzutti CS, Rohan LC. Targeted delivery of PSC-Rantes for HIV-1 prevention using biodegradable nanoparticles. *Pharm Res* 2009;**26**:502-11.
- Zhang T, Sturgis TF, Youan BB. pH-responsive nanoparticles releasing tenofovir intended for the prevention of hiv transmission. *Pharm Biopharm* 2011;**79**:526-36.
- das Neves J, Michiels J, Arien KK, Vanham G, Amiji M, Bahia MF, et al. Polymeric nanoparticles affect the intracellular delivery, antiretroviral activity and cytotoxicity of the microbicide drug candidate dapivirine. *Pharm Res* 2012;**29**:1468-84.
- das Neves J, Amiji M, Bahia MF, Sarmento B. Assessing the physical-chemical properties and stability of dapivirine-loaded polymeric nanoparticles. *Pharm* 2013;**456**:307-14.
- Lackman-Smith C, Osterling C, Luckenbaugh K, Mankowski M, Snyder B, Lewis G, et al. Development of a comprehensive human immunodeficiency virus type 1 screening algorithm for discovery and preclinical testing of topical microbicides. *Antimicrob Agents Chemother* 2008;**52**:1768-81.

16. Dezzutti CS. Animal and human mucosal tissue models to study HIV biomedical interventions: can we predict success? *Soc* 2015;**18**:20301.
17. Olesen R, Wahl A, Denton PW, Garcia JV. Immune reconstitution of the female reproductive tract of humanized blt mice and their susceptibility to human immunodeficiency virus infection. *J Reprod Immunol* 2011;**88**:195-203.
18. Novikov MS, Ivanova ON, Ivanov AV, Ozerov AA, Valuev-Elliston VT, Temburnikar K, et al. 1-[2-(2-benzoyl- and 2-benzylphenoxy)ethyl]juracils as potent anti-HIV-1 agents. *Bioorg Med Chem* 2011;**19**:5794-802.
19. Prokofjeva MM, Spirin PV, Yanvarev DV, Ivanov AV, Novikov MS, Stepanov OA, et al. Screening of potential hiv-1 inhibitors/replication blockers using secure lentiviral in vitro system. *Acta Nat* 2011;**3**:55-65.
20. Bogdanov Jr A, Gupta S, Koshkina N, Corr SJ, Zhang S, Curley SA, et al. Gold nanoparticles stabilized with mpeg-grafted poly(l-lysine): in vitro and in vivo evaluation of a potential theranostic agent. *Bioconjug Chem* 2015;**26**:39-50.
21. Reichstetter S, Castillo GM, Lai MS, Nishimoto-Ashfield A, Banerjee A, Bogdanov Jr A, et al. Protected graft copolymer (pgc) basal formulation of insulin as potentially safer alternative to Lantus® (insulin-glargine): a streptozotocin-induced, diabetic Sprague dawley rats study. *Pharm Res* 2012;**29**:1033-9.
22. Van Gysegem E, Pendela M, Baert L, Rosier J, Van 't Klooster G, De Man H, et al. Powder for reconstitution of the anti-HIV-1 drug TMC278 - formulation development, stability and animal studies. *Pharm Biopharm* 2008;**70**:853-60.
23. Usach I, Melis V, Peris JE. Non-nucleoside reverse transcriptase inhibitors: a review on pharmacokinetics, pharmacodynamics, safety and tolerability. *Soc* 2013;**16**:1-14.
24. Castillo GM, Reichstetter S, Bolotin EM. Extending residence time and stability of peptides by protected graft copolymer (PGC) excipient: GLP-1 example. *Pharm Res* 2012;**29**:306-18.
25. Bogdanov AA, Mazzanti M, Castillo G, Bolotin E. Protected graft copolymer (PGC) in imaging and therapy: a platform for the delivery of covalently and non-covalently bound drugs. *Theranostics* 2012;**2**:553-76.
26. Lai SK, O'Hanlon DE, Harrold S, Man ST, Wang YY, Cone R, et al. Rapid transport of large polymeric nanoparticles in fresh undiluted human mucus. *S A* 2007;**104**:1482-7.
27. Ensign LM, Schneider C, Suk JS, Cone R, Hanes J. Mucus penetrating nanoparticles: biophysical tool and method of drug and gene delivery. *Adv Mater* 2012;**24**:3887-94.
28. Platt EJ, Wehrly K, Kuhmann SE, Chesebro B, Kabat D. Effects of CCR5 and CD4 cell surface concentrations on infections by macrophagetropic isolates of human immunodeficiency virus type 1. *J Virol* 1998;**72**:2855-64.
29. Wei X, Decker JM, Liu H, Zhang Z, Arani RB, Kilby JM, et al. Emergence of resistant human immunodeficiency virus type 1 in patients receiving fusion inhibitor (T-20) monotherapy. *Antimicrob Agents Chemother* 2002;**46**:1896-905.
30. Li W, Wang Q, Li Y, Yu F, Liu Q, Qin B, et al. A nanoparticle-encapsulated non-nucleoside reverse-transcriptase inhibitor with enhanced anti-HIV-1 activity and prolonged circulation time in plasma. *Curr Pharm Des* 2015;**21**:925-35.
31. Greenhead P, Hayes P, Watts PS, Laing KG, Griffin GE, Shattock RJ. Parameters of human immunodeficiency virus infection of human cervical tissue and inhibition by vaginal virucides. *J Virol* 2000;**74**:5577-86.
32. Denton PW, Othieno F, Martinez-Torres F, Zou W, Krisko JF, Fleming E, et al. One percent tenofovir applied topically to humanized BLT mice and used according to the caprisa 004 experimental design demonstrates partial protection from vaginal HIV infection, validating the BLT model for evaluation of new microbicide candidates. *J Virol* 2011;**85**:7582-93.
33. Kang H, Weissleder R, Bogdanov Jr A. Targeting of MPEG-protected polyamino acid carrier to human E-selectin in vitro. *Amino Acids* 2002;**23**:301-8.